

# Nonlinear manipulation and control of matter waves

E. V. Goldstein, M. G. Moore and P. Meystre

*Optical Sciences Center and Department of Physics, University of Arizona, Tucson, AZ 85721*

This paper reviews some of our recent results in nonlinear atom optics. In addition to nonlinear wave-mixing between matter waves, we also discuss the dynamical interplay between optical and matter waves. This new paradigm, which is now within experimental reach, has the potential to impact a number of fields of physics, including the manipulation and applications of atomic coherence, and the preparation of quantum entanglement between microscopic and macroscopic systems. Possible applications include quantum information processing, matter-wave holography, and nanofabrication.

## I. INTRODUCTION

The last few years have been exciting ones indeed for atomic, molecular and optical physics. Advances have been spectacular, both on the theoretical and the experimental front, and many of the ideas which were “far-off” proposals just a few years back have now become reality. This is in particular the case for “atom lasers” and nonlinear atom optics. Since the first demonstration of a primitive atom laser by Ketterle and coworkers [1], at least three other systems have been demonstrated [2–4], including a quasi-cw system by the group of Hänsch [4], and a “mode-locked” system by Kasevich [2]. Just as important was the experimental demonstration of matter-wave four-wave mixing by Phillips’ group at NIST [5], and shortly thereafter of matter-wave superradiance by Ketterle’s group [6]. In addition, there is an exciting convergence of interests taking place between Bose-Einstein condensation and the study of quantum-coherent effects such as echoes [7] and electromagnetic induced transparency (EIT), demonstrated spectacularly in the recent experiments of Hau et al [8] and others [9].

Any potential application of quantum degenerate gases will rely on one’s ability to manipulate and control them. One obvious way to do that is by optical methods: It has long been known that optical fields can be used as atom-optical elements [10], for instance as diffraction gratings. They can work just as well for condensates, and indeed, Phillips and coworkers [11,5] used them in their trailblazing nonlinear atom optics experiments to prepare three of the matter waves that were then used to generate a fourth one. Optical waves can also be used to produce optical dipole traps, which have played a central role in the studies of multicomponent condensates by the MIT group [6]. As a final example, we can mention the use of an optical lattice to build a “mode-locked” atom laser by Kasevich and coworkers [2].

In this first generation of applications, the light field

played a passive role: it influenced the dynamics of the matter waves, but the back-action of the atomic field on the optical field was largely neglected. In recent work, we [12–14] and others [15–17] have introduced a new paradigm where both the optical and the matter waves are dynamically coupled, independent entities.

The remainder of this paper reviews some recent results obtained by our group in nonlinear atom optics. Section II discusses a situation where atoms in a multicomponent condensate interact via spin-changing collisions. We show how the dynamics of this system is characterized by the occurrence of collapses and revivals in the population of the various magnetic sublevels involved. Section III considers the nonlinear mixing of optical and matter waves, and illustrates the optical control of the coherence properties of a quantum-degenerate atomic gas. Potential applications of atom optics are numerous, and just starting to be explored, as an outlook into the future, Section IV briefly reviews just one such potential application, atom holography.

## II. NONLINEAR ATOM OPTICS

Several years ago, we proposed the idea of nonlinear atom optics [18,19]. A number of theoretical investigations along these lines have now been carried out, including the study of matter-wave solitons [19–24], phase conjugation [25–27], four-wave mixing [28], etc.

In that context, the coexistence of condensates with different magnetic quantum numbers is attractive in that it provides a way to perform four-wave mixing experiments in collinear geometries [27], thereby eliminating phase-matching limitations. As an illustration, consider a Bose-Einstein condensate of  $^{23}\text{Na}$  atoms in the  $F = 1$  hyperfine ground state, with the three internal atomic states  $|F = 1, m = -1\rangle$ ,  $|F = 1, m = 0\rangle$  and  $|F = 1, m = 1\rangle$  of degenerate energies in the absence of external magnetic fields. The condensate is confined by a far-off-resonant optical dipole trap. It is described by the three-component Schrödinger vector field

$$\Psi(\mathbf{r}, t) = \{\Psi_{-1}(\mathbf{r}, t), \Psi_0(\mathbf{r}, t), \Psi_1(\mathbf{r}, t)\} \quad (1)$$

which satisfies the bosonic commutation relations

$$[\Psi_i(\mathbf{r}, t), \Psi_j^\dagger(\mathbf{r}', t)] = \delta_{ij}\delta(\mathbf{r} - \mathbf{r}'). \quad (2)$$

Accounting for the possibility of two-body collisions, its dynamics is described by the second-quantized Hamiltonian

$$\mathcal{H} = \int d\mathbf{r} \Psi^\dagger(\mathbf{r}, t) H_0 \Psi(\mathbf{r}, t) + \frac{1}{2} \int \int d\mathbf{r}_1 d\mathbf{r}_2 \times \Psi^\dagger(\mathbf{r}_1, t) \Psi^\dagger(\mathbf{r}_2, t) V(\mathbf{r}_1 - \mathbf{r}_2) \Psi(\mathbf{r}_2, t) \Psi(\mathbf{r}_1, t), \quad (3)$$

where the single-particle Hamiltonian is

$$H_0 = \mathbf{p}^2/2M + V_{trap} \quad (4)$$

and the trap potential is of the general form

$$V_{trap} = \sum_{m=-1}^{+1} U(\mathbf{r}) |F=1, m\rangle \langle F=1, m|. \quad (5)$$

Here  $\mathbf{p}$  is the center-of-mass momentum of the atoms of mass  $M$  and  $U(\mathbf{r})$ , the effective dipole trap potential for atoms in the  $|F=1, m\rangle$  hyperfine state, is independent of  $m$  for a non-magnetic trap.

Considering situations where the hyperfine spin  $F_i = 1$  of the individual atoms is preserved during collisions, it can be shown that in the shapeless approximation the two-body interaction is [29,30]

$$V(\mathbf{r}_1 - \mathbf{r}_2) = \hbar\delta(\mathbf{r}_1 - \mathbf{r}_2) (c_0 + c_2 \mathbf{F}_1 \cdot \mathbf{F}_2), \quad (6)$$

where  $c_0 = (g_0 + 2g_2)/3$  and  $c_2 = (g_2 - g_0)/3$ , where

$$g_f = 4\pi\hbar a_f/M, \quad (7)$$

Here we label the hyperfine states of the combined system of two collision partners with total hyperfine spin  $\mathbf{F} = \mathbf{F}_1 + \mathbf{F}_2$  by  $|f, m\rangle$ , where  $f = 0, 1, 2$  and  $m = -f, \dots, f$  and  $a_f$  is the  $s$ -wave scattering length for the channel of total hyperfine spin  $f$ . Substituting this form into the second-quantized Hamiltonian (3) leads to

$$\begin{aligned} \mathcal{H} = & \sum_m \int d\mathbf{r} \Psi_m^\dagger(\mathbf{r}, t) \left[ \frac{\mathbf{p}^2}{2M} + U(\mathbf{r}) \right] \Psi_m(\mathbf{r}, t) \\ & + \frac{\hbar}{2} \int d\mathbf{r} \{ (c_0 + c_2) [\Psi_1^\dagger \Psi_1^\dagger \Psi_1 \Psi_1 + \Psi_{-1}^\dagger \Psi_{-1}^\dagger \Psi_{-1} \Psi_{-1}] \\ & + 2\Psi_0^\dagger \Psi_0 (\Psi_1^\dagger \Psi_1 + \Psi_{-1}^\dagger \Psi_{-1}) + c_0 \Psi_0^\dagger \Psi_0^\dagger \Psi_0 \Psi_0 \\ & + 2(c_0 - c_2) \Psi_1^\dagger \Psi_1 \Psi_{-1}^\dagger \Psi_{-1} \\ & + 2c_2 (\Psi_1^\dagger \Psi_{-1}^\dagger \Psi_0 \Psi_0 + H.c.) \}. \end{aligned} \quad (8)$$

The three terms quartic in one of the field operators only, i.e. of the form  $\Psi_i^\dagger \Psi_i^\dagger \Psi_i \Psi_i$  are self-defocussing terms, the terms involving two hyperfine states conserve the populations of the individual spin states and merely lead to phase shifts, and the terms involving the central mode  $\Psi_0$  and *both* side-modes correspond to spin-exchange collisions. This ‘‘four-wave mixing’’ interaction, involving e.g. the annihilation of a pair of atoms with  $m_F = 0$  and the creation of two atoms in the states  $m_F = \pm 1$ , leads to phase conjugation in quantum optics and to matter-wave phase conjugation in the present case. [27]

The analogy with optical four-wave mixing becomes even more apparent when we consider a situation where

atoms in the  $m_F = 0$  state are placed in a linear superposition of two counterpropagating center-of-mass modes of momenta  $\pm \hbar k_0$ , that is

$$\Psi_0(x) = \frac{1}{\sqrt{V}} (e^{ik_0 x} a_{01} + e^{-ik_0 x} a_{02}), \quad (9)$$

while the atoms of spin  $m_F = \pm 1$  are taken to be the running waves

$$\Psi_{\pm 1}(x) = \frac{1}{\sqrt{V}} e^{\pm ik_0 x} a_{\pm 1}. \quad (10)$$

Here  $a_{01}$  and  $a_{02}$  are the annihilation operators of the two counterpropagating  $m_F = 0$  modes, with  $[a_{0i}, a_{0j}^\dagger] = \delta_{ij}$ ,  $i, j = 1$  or  $2$ , and  $a_1, a_{-1}$  are the corresponding operators for the running modes associated with  $m_F = \pm 1$ . Finally,  $V$  is the confinement volume of the condensate. Inserting this mode expansion into the Hamiltonian (8) and ignoring all non-phase-matched contributions yields the four-wave mixing Hamiltonian

$$\begin{aligned} \mathcal{H} = & \frac{\hbar^2 k_0^2}{2M} \hat{N} + \frac{\hbar c_0}{2} \hat{N}(\hat{N} - 1) \\ & + \frac{\hbar c_2}{2} (a_1^\dagger a_1^\dagger a_1 a_1 + a_{-1}^\dagger a_{-1}^\dagger a_{-1} a_{-1} - 2a_1^\dagger a_1 a_{-1}^\dagger a_{-1} \\ & + 2(a_1^\dagger a_1 + a_{-1}^\dagger a_{-1})(a_{01}^\dagger a_{01} + a_{02}^\dagger a_{02}) \\ & + 4a_1^\dagger a_{-1}^\dagger a_{01} a_{02} + 4a_1 a_{-1} a_{01}^\dagger a_{02}^\dagger), \end{aligned} \quad (11)$$

where we have introduced the total number of atoms  $\hat{N} = \hat{N}_1 + \hat{N}_2$ ,  $\hat{N}_1 = a_1^\dagger a_1 + a_{01}^\dagger a_{01}$  and  $\hat{N}_2 = a_{-1}^\dagger a_{-1} + a_{02}^\dagger a_{02}$ .

This problem was solved exactly in Ref. [28] using an angular momentum representation. Here, we reproduce just one result of this analysis for illustration. We consider for concreteness a condensate consisting of  $N$  atoms such that there are initially  $N_1 = N_2 = N/2$ , with  $m \ll N/2$  atoms in the hyperfine state  $m_F = 1$  and none in the state  $m_F = 0$ . The evolution of the population of the  $m_F = 1$  sidemode is shown in Fig. 1 for  $N = 100$  atoms in the system. In case (b) the initial mode population is  $\langle a_1^\dagger a_1 \rangle = m = 5$ , while case (a) illustrates the build-up from noise,  $m = 0$ . In both cases, the sidemode population exhibits an initial growth to the point where it contains about 1/3 of the atoms in the first case and about half of the atoms in the second. This is followed by a collapse to a quasi-steady state population, as well as a subsequent revival at  $2c_2 t_1 = \pi$ . This dynamics then repeats itself periodically, with revivals at  $2c_2 t_n = \pi n$ , independently of  $N$ .

In analogy with the optical case, matter-wave four-wave mixing is expected to lead to the quantum entanglement of the condensate sidemodes. One can quantify the amount of entanglement by determining the extent to which the Cauchy-Schwartz inequality is violated by the second-order cross-correlation functions between modes. Our results [28] show that the correlations between central mode and sidemodes satisfy the classical Cauchy-Schwartz inequality, while the sidemode—sidemode cross correlations violate them.

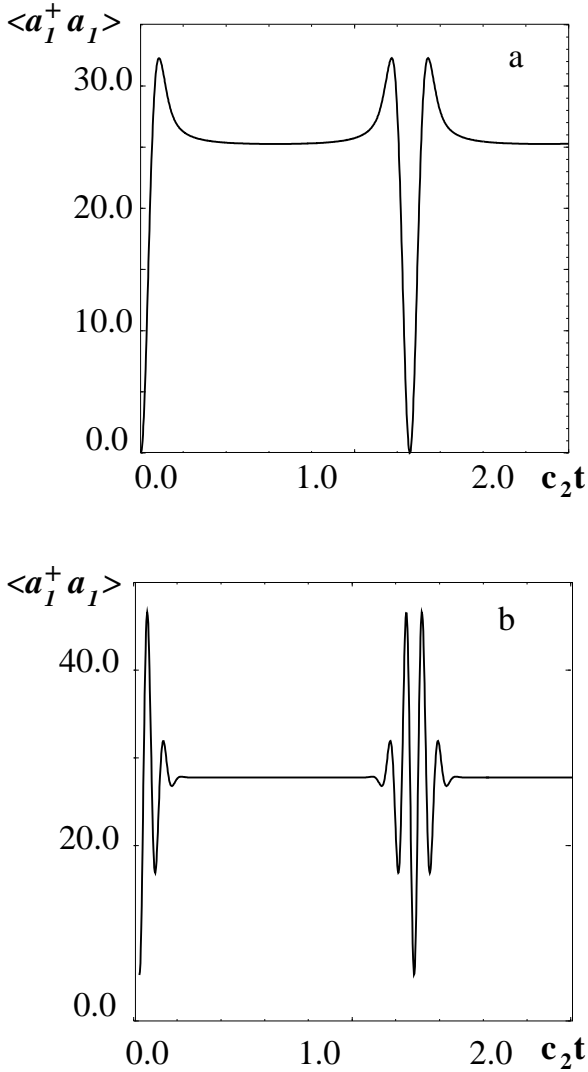


FIG. 1. Time evolution of the side-mode population  $\langle a_1^\dagger a_1 \rangle$  for  $N=100$  and initial populations (a)  $\langle a_{01}^\dagger a_{01} \rangle = N/2$ ,  $\langle a_{02}^\dagger a_{02} \rangle = N/2$ ,  $\langle a_1^\dagger a_1 \rangle = 0$  and  $\langle a_{-1}^\dagger a_{-1} \rangle = 0$  (b)  $\langle a_{01}^\dagger a_{01} \rangle = N/2 - 5$ ,  $\langle a_{02}^\dagger a_{02} \rangle = N/2$ ,  $\langle a_1^\dagger a_1 \rangle = 5$  and  $\langle a_{-1}^\dagger a_{-1} \rangle = 0$ . (After Ref. [28].)

The violation is particularly strong in the case of build-up from noise, as should be intuitively expected. The difference in the behavior of the two-mode correlation functions between side-modes and those involving one central and one side-mode can be intuitively understood from the form of the wave-mixing term  $a_1^\dagger a_{-1}^\dagger a_{01} a_{02}$  appearing in the Hamiltonian (11). Indeed, the coupling between side-modes, involving two annihilation operators, is reminiscent of the interaction  $a_1^\dagger a_2^\dagger$  in the Hamiltonian of parametric amplification leading to squeezing and quantum entanglement between two sidemodes. In contrast, the coupling between central and sidemodes involves both an annihilation and a creation operator.

### III. OPTICAL AND MATTER-WAVE MIXING

As we have seen in section II, the matter-wave optics analog of a nonlinear optical medium is provided by collisions. In particular, two-body collisions in the shapeless approximation are mathematically equivalent to a local Kerr medium with instantaneous response. These collisions result from the elimination of the continuum of modes of the electromagnetic field from the dynamics, very much like the elimination of the material dynamics leads to nonlinear optics.

This section turns to an intermediate regime where neither the matter waves nor the electromagnetic field can be eliminated. In this case, it becomes in particular possible to optically manipulate and control the quantum statistics of matter waves (and conversely). We illustrate how this works in the specific example of an ultracold sample of bosonic atoms located inside an optical ring cavity and driven by a strong classical “pump” and a counterpropagating weak quantized “probe” optical field. Both fields are assumed to be far off-resonant from any electronic transition, so that all excited states can be adiabatically eliminated from the dynamics, and the matter-wave field is effectively scalar.

The combined Hamiltonian for the atomic and probe fields is

$$\begin{aligned} \hat{H} = & \frac{\hbar^2}{2m} \sum_{\mathbf{q}} q^2 \hat{c}^\dagger(\mathbf{q}) \hat{c}(\mathbf{q}) + \hbar c k \hat{A}^\dagger \hat{A} \\ & + i \frac{\hbar}{2\Delta} \sum_{\mathbf{q}} \left[ g \Omega_0 e^{-i\omega_0 t} \hat{A}^\dagger \hat{c}^\dagger(\mathbf{q} - \mathbf{K}) \hat{c}(\mathbf{q}) - H.c. \right] \\ & + \frac{\hbar}{\Delta} \left( \frac{|\Omega_0|^2}{4} + |g|^2 \hat{A}^\dagger \hat{A} \right) \sum_{\mathbf{q}} \hat{c}^\dagger(\mathbf{q}) \hat{c}(\mathbf{q}). \end{aligned} \quad (12)$$

Here,  $\Omega_0$  is the Rabi frequency of the pump laser of frequency  $\omega_0$  and momentum  $\mathbf{k}_0$ ,  $\hat{A}$  is the annihilation operator of the probe field of frequency  $\omega$  and momentum  $\mathbf{k}$ , satisfying  $[\hat{A}, \hat{A}^\dagger] = 1$ , and  $\hat{c}(\mathbf{q})$  is the annihilation operator for a ground state atom of momentum  $\mathbf{q}$ , satisfying  $[\hat{c}(\mathbf{q}), \hat{c}^\dagger(\mathbf{q}')] = \delta_{\mathbf{q}, \mathbf{q}'}$ . In addition,  $\Delta$  is the detuning between the pump frequency and the upper electronic level closest to resonance, and  $g = d[ck/(2\hbar\epsilon_0 LS)]^{1/2}$  is the atom-probe coupling constant,  $d$  is the atomic dipole moment,  $L$  the length of the ring cavity, and  $S$  the cross-section of the probe mode in the region of the atomic sample. Finally,  $\mathbf{K} \equiv \mathbf{k} - \mathbf{k}_0$  is the atomic recoil momentum resulting from the absorption of a pump photon followed by the emission of a probe photon.

The first two terms in Eq. (12) are the free Hamiltonians of the atomic and probe fields, respectively. The remaining terms correspond to the various processes by which an atom undergoes a virtual transition under the influence of the optical fields. The first such term involves the exchange of a photon between the pump and probe fields, e.g. stimulated absorption of a pump photon followed by stimulated emission of a probe photon,

or vice versa. The last two terms correspond to processes where a photon is first absorbed and then reemitted into the same field. These transitions are recoilless, but contribute a cross-phase modulation between the atomic and optical fields.

Assuming that the initial momentum width of the condensate is small compared to the recoil momentum  $K$ , it is reasonable to treat it as a *single mode* atomic field of momentum  $\mathbf{q} = 0$ . We furthermore restrict our discussion to the case  $T \ll T_c$ , where  $T_c$  is the critical temperature, and assume a large condensate for which the bare mode  $q = 0$  can be described to a good approximation as a *c-number*,  $\hat{c}(0) \rightarrow \sqrt{N} \exp(i|\Omega_0|^2 t/4\Delta)$ , where  $N$  is the mean number of atoms in the condensate. This approximation neglects both the depletion which occurs as atoms are transferred into the side-modes  $q \neq 0$  and the cross-phase modulation between the condensate and the probe field, thus it is valid for times short enough that  $\sum_{\mathbf{q} \neq 0} \langle \hat{c}^\dagger(\mathbf{q}) \hat{c}(\mathbf{q}) \rangle \ll N$ , and  $\langle \hat{A}^\dagger \hat{A} \rangle \ll |\Omega_0|^2/4|g|^2$ . This is the matter-wave optics analog of the familiar classical and undepleted pump approximation of nonlinear optics. Hence we describe the optical and matter-wave fields on equal footings, treating all strongly populated modes classically and all weakly populated modes quantum-mechanically. The growth of the system can be triggered either from vacuum fluctuations, as we discuss in more detail shortly, or by a weak injected probe signal.

Once we have replaced the condensate mode with its *c-number* counterpart, we neglect all terms in the Hamiltonian (12) involving the product of three or more weakly populated modes. This yields the effective Hamiltonian

$$\begin{aligned} \hat{H} = \hbar\omega_r & \left[ \hat{c}_+^\dagger \hat{c}_+ + \hat{c}_-^\dagger \hat{c}_- - \delta \hat{a}^\dagger \hat{a} \right. \\ & \left. + \chi \left( \hat{a}^\dagger \hat{c}_-^\dagger + \hat{a}^\dagger \hat{c}_+ + \hat{c}_+^\dagger \hat{a} + \hat{c}_- \hat{a} \right) \right], \end{aligned} \quad (13)$$

where  $\omega_r = \hbar K^2/2m$ , and we have introduced the slowly varying operators  $\hat{c}_\pm = \exp(i|\Omega_0|^2 t/4\Delta) \hat{c}(\pm \mathbf{K})$  and  $\hat{a} = -i(g^* \Omega_0^* \Delta / |g| |\Omega_0| |\Delta|) \exp(i\omega_0 t) \hat{A}$ . The system is fully characterized by the effective coupling constant  $\chi = |g| |\Omega_0| \sqrt{N} / 2\omega_r \Delta$  and the dimensionless pump-probe detuning  $\delta = (\omega_0 - \omega) / \omega_r$ .

The Hamiltonian (13) describes three coupled field modes: the optical probe and two atomic condensate side-modes with wavenumbers  $\pm \mathbf{K}$ . The term  $\hat{a}^\dagger \hat{c}_-^\dagger$  in Eq. (13) describes the creation of correlated atom-photon pairs, and immediately brings to mind the optical parametric amplifier [31], a device known to generate highly non-classical optical fields exhibiting two-mode intensity correlations and squeezing, and which has been extensively employed in the creation of entangled photon pairs for fundamental studies of quantum mechanics, quantum cryptography and quantum computing. A novel aspect of the present system is that it offers a way to achieve quantum entanglement between atomic and optical fields.

We concentrate here on the equal-time two-mode intensity cross-correlations, which are a measure of the

degree of entanglement between the modes of the system. For example, the intensity cross-correlation function  $g_{a-}^{(2)}(\tau)$  is defined as

$$g_{a-}^{(2)} = \frac{\langle \hat{a}^\dagger(\tau) \hat{a}(\tau) \hat{c}_-^\dagger(\tau) \hat{c}_-(\tau) \rangle}{\langle \hat{a}^\dagger(\tau) \hat{a}(\tau) \rangle \langle \hat{c}_-^\dagger(\tau) \hat{c}_-(\tau) \rangle}. \quad (14)$$

Other intensity cross-correlation functions such as  $g_{a+}^{[2]}(\tau)$  and  $g_{-+}^{(2)}(\tau)$  are defined similarly. For classical fields, there is an upper limit to the second-order equal-time correlation function. It is given by the Cauchy-Schwartz inequality [31]

$$g_{ij}^{(2)}(\tau) \leq \left[ g_i^{(2)}(\tau) \right]^{1/2} \left[ g_j^{(2)}(\tau) \right]^{1/2}. \quad (15)$$

Quantum mechanical fields, however, can violate this inequality and are instead constrained by [31]

$$g_{ij}^{(2)}(\tau) \leq \left[ g_i^{(2)}(\tau) + \frac{1}{I_i(\tau)} \right]^{1/2} \left[ g_j^{(2)}(\tau) + \frac{1}{I_j(\tau)} \right]^{1/2}, \quad (16)$$

which reduces to the classical result in the limit of large intensities.

Consider first the ‘‘spontaneous’’ case where the pump field is initially in a vacuum. In this case, the equal-time intensity cross-correlation functions are found to be

$$\begin{aligned} g_{a-}^{(2)} = g_{-+}^{(2)} &= \left[ 2 + \frac{1}{I_a(\tau) + I_+(\tau)} \right]^{1/2} \left[ 2 + \frac{1}{I_-(\tau)} \right]^{1/2}, \\ g_{a+}^{(2)} &= 2. \end{aligned} \quad (17)$$

Ref. [14] shows that both  $g_{a-}^{(2)}(\tau)$  and  $g_{-+}^{(2)}(\tau)$  violate the Cauchy-Schwartz inequality, while  $g_{a+}^{(2)}(\tau)$  is consistent with classical cross-correlations. Furthermore,  $g_{a-}^{(2)}(\tau)$  is very close to the maximum violation of the classical inequality consistent with quantum mechanics, whereas for  $g_{-+}^{(2)}(\tau)$  the violation is not close to the allowed maximum. In the two-mode parametric amplifier of quantum optics, the two-mode correlation function shows the maximum violation of the Cauchy-Schwartz inequality consistent with quantum mechanics. In the present three-mode system, however, the two-mode cross-correlation functions involve a trace over the third mode, hence it is not surprising that the two-mode correlations are not maximized.

If we now allow for an injected coherent probe field, we find that in contrast to the ‘‘spontaneous’’ case,  $g_{a-}^{(2)}$  now lies somewhere in between the quantum (16) and classical (15) limits. As the strength of the classical probe field is increased, this correlation falls ever closer to the classical upper limit, so that in the limit of very large probe fields, one finds classical cross-correlations only.

These results show that the quantum state of momentum side-modes of a condensate can be varied continuously between two distinct limits by specifying the initial state of an optical cavity mode. When it begins in the vacuum state, the side-mode and the cavity mode fields develop with zero mean fields, thermal intensity fluctuations, and strong quantum correlations between the modes. In contrast, when it is prepared in strong coherent state, we approach a “classical” limit in which the fields develop with non-zero mean fields having well defined phases, intensity fluctuations indicating a coherent state, and exhibiting classical correlations only.

#### IV. OUTLOOK — ATOM HOLOGRAPHY

The interplay between optical and matter waves opens up intriguing possibilities, such as matter-wave holography, to which we now turn. Optical holography can be described as the three-dimensional reconstruction of the optical image of an arbitrarily shaped object. Typically, this is done in a two-step process where first the information about the object is stored in a hologram. This hologram is created by recording, e.g., with the help of a photographic film, the interference pattern between scattered light originating from the illuminated object and a (plane-wave) reference beam. The second step is the reconstruction, which is performed by shining a reading beam similar to the reference beam onto the hologram. The diffraction of the reading beam from the recorded pattern yields a virtual as well as a real optical image of the original object.

Drawing on this concept, the characteristic property of atomic holography is that at least the final reading step is performed with an atomic beam. In this way, an atom-optical image of the object is created which in certain situations can be thought of as some sort of material replica of the original. Such replicas may have useful practical applications from atom lithography to the manufacturing of microstructures, or quantum microfabrication.

One of the prerequisites for an actual implementation of atomic holography is the availability of a reading beam of sufficient monochromaticity and coherence. Given the rapid advances in atom optics and especially in the realization of atom lasers, this requirement can be expected to be met in the near future. One of the greatest challenges, however, is the manufacturing of the actual hologram where the information to be reconstructed is stored. Several schemes can be considered. One possibility is to diffract the atoms from a mechanical mask. The first successful realizations of such an approach have recently been reported in Ref. [32]. In these experiments the hologram was manufactured as a binary mask written onto a thin silicon nitride membrane. Such a hologram has the advantage of being permanent, however, as the mask only allows for complete or vanishing (binary) transmission of the beam at a given point one loses a significant

amount of information about the optical image. Another interesting proposal was recently made in Ref. [33]. In this setup the atomic beam is diffracted from the inhomogeneous light field created by the superposition of object and reference beam. These beams thus directly form the hologram.

In our approach, in contrast, the holographic information is encoded into the condensate in the form of density modulations by using writing and reference laser beams that form an optical potential for the condensate atoms. All-atomic reading is then accomplished in a way reminiscent of the Raman-Nath regime of diffraction between an atomic beam and a light field. [10] Specifically, the reading beam atoms, that have a suitably chosen velocity, interact with the condensate atoms via  $s$ -wave scattering and acquire a spatially dependent phase shift reflecting the density modulations of the condensate. In the further spatial propagation of the atoms, this phase shift gives rise to the formation of the atom-optical image.

The idea of storing information in atomic condensates is based on the observation that the density distribution of a condensate in the Thomas-Fermi limit closely reflects the behavior of the confining potential. This yields the possibility of accurate external control. The Gross-Pitaevskii equation which governs the evolution of the macroscopic wave function  $\Phi(\mathbf{r}, t)$  describing the state of an atomic condensate with  $N$  atoms is given by [34]

$$i\hbar\dot{\Phi} = \frac{\mathbf{p}^2}{2M}\Phi + V(\mathbf{r})\Phi + g|\Phi|^2\Phi, \quad (18)$$

where  $\mathbf{p}$  denotes the atomic center-of-mass momentum,  $M$  the atomic mass, and  $V(\mathbf{r})$  the external potential. The strength of atomic two-body interactions is determined by  $g = 4\pi\hbar^2 a/M$  with  $a$  being the  $s$ -wave scattering length. The normalization condition for the condensate wave function reads

$$\int d^3\mathbf{r} |\Phi(\mathbf{r})|^2 = N. \quad (19)$$

The steady state of a condensate can thus be described with a wave function  $\Phi(\mathbf{r}, t) = \exp(-i\mu t/\hbar)\phi(\mathbf{r})$ , with  $\mu$  being the chemical potential determined by the normalization condition Eq. (19).

In the Thomas-Fermi limit, where the effect of kinetic energy is much weaker than the mean-field potential, the contribution of the term  $\mathbf{p}^2/2M$  can be neglected and the condensate density becomes

$$|\phi(\mathbf{r})|^2 = [\mu - V(\mathbf{r})]/g, \quad (20)$$

From this expression we see immediately that the form of the external potential is replicated in the density profile of the atomic condensate.

For reading, we consider an all-atomic scheme which has the fundamental advantage of allowing one to reconstruct a *material* “replica” of the stored object. Specifically, the reading beam is a monoenergetic atomic beam

of velocity  $\mathbf{v}_{rd}$  impinging at some angle onto the condensate. We assume that the internal state of these incoming atoms is such that they are only weakly perturbed by the writing and trap potentials, so that their dominant interaction is scattering by the atoms in the condensate. It is important at this point to emphasize that the atoms in the reading beam *need not* be of the same species as the condensate atoms. In principle they could be of just about any element or even molecule.

Fig. 2 shows an example, taken from Ref. [35], which demonstrates explicitly that an original rectangular aperture can be indeed reconstructed with our proposed atom holography method.

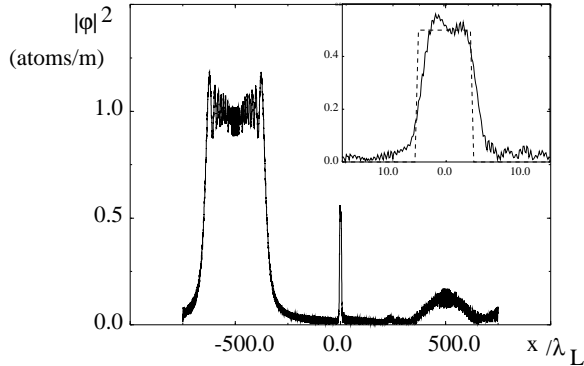


FIG. 2. Reconstructing a replica of the original object from the atomic hologram. The reading beam consists of a monochromatic beam of sodium atoms moving at an angle  $\beta_A$  from the  $z$  axis at a velocity  $v_{rd} = 0.1$  m/sec. Shown is the atomic density profile at a distance  $\Delta z$  from the condensate such that the quadratic phase shift of the conjugate image is precisely canceled. The insert compares the reconstructed and original objects. The off-axis feature for positive  $x$  corresponds to the real object, for which the quadratic phase is still present. The large off-axis feature at negative  $x$  is the background. (After Ref. [35].)

#### ACKNOWLEDGMENTS

This work is supported in part by the U.S. Office of Naval Research under Contract No. 14-91-J1205, by the National Science Foundation under Grant No. PHY98-01099, by the U.S. Army Research Office, and by the Joint Services Optics Program.

[1] M.-O. Mewes *et al.*, Phys. Rev. Lett. **78**, 582 (1997).

[2] B. P. Anderson and M. A. Kasevich, Science **282**, 1686 (1998).

[3] E. W. Hagley *et al.*, Science **283**, 1706 (1999).

[4] I. Bloch, T. W. Hänsch, and T. Esslinger, Phys. Rev. Lett. **82**, 3008 (1999).

[5] L. Deng *et al.*, Nature **398**, 218 (1999).

[6] S. Inouye *et al.*, unpublished (1999).

[7] A. B. Kuklov and N. Chencinski, Phys. Rev. A **57**, 4699 (1998).

[8] L. V. Hau, S. E. Harris, Z. Dutton, and C. H. Behroozi, Nature **397**, 594 (1999).

[9] M. M. Kash *et al.*, Phys. Rev. Lett. **82**, in press (1999).

[10] C. S. Adams, M. Sigel, and J. Mlynek, Physics Reports **240**, 143 (1994).

[11] M. Kozuma *et al.*, Phys. Rev. Lett. **82**, 871 (1999).

[12] M. G. Moore and P. Meystre, Phys. Rev. A **58**, 3248 (1998).

[13] M. G. Moore and P. Meystre, Phys. Rev. A **59**, R1754 (1999).

[14] M. G. Moore, O. Zobay, and P. Meystre, Phys. Rev. A **60**, (1999).

[15] H. Zeng, F. Lin, and W. Zhang, Phys. Lett. A **201**, 397 (1995).

[16] C. K. Law and N. P. Bigelow, Phys. Rev. A **58**, 4791 (1998).

[17] L. Kuang, Commun. Theor. Phys. **30**, 161 (1998).

[18] G. Lenz, P. Meystre, and E. W. Wright, Phys. Rev. Lett. **71**, 3271 (1993).

[19] G. Lenz, P. Meystre, and E. W. Wright, Phys. Rev. A **50**, 1681 (1994).

[20] S. A. Morgan, R. J. Ballagh, and K. Burnett, Phys. Rev. A **55**, 4338 (1997).

[21] W. P. Reinhardt and C. W. Clark, J. Phys. B **30**, L785 (1997).

[22] R. Dum, J. I. CiracM., Lewenstein, and P. Zoller, Phys. Rev. Lett. **80**, 2972 (1998).

[23] A. D. Jackson, G. M. Kavoulakis, and C. J. Pethick, Phys. Rev. A **58**, 2417 (1998).

[24] O. Zobay, S. Pötting, E. M. Wright, and P. Meystre, Phys. Rev. A **59**, 643 (1999).

[25] E. V. Goldstein, K. Plättner, and P. Meystre, Quant. Semiclas. Optics **7**, 743 (1995).

[26] E. V. Goldstein, K. Plättner, and P. Meystre, Jrnl. Res. Nat. Inst. Stand. Technol. **101**, 583 (1996).

[27] E. V. Goldstein and P. Meystre, Phys. Rev. A **59**, 1509 (1999).

[28] E. V. Goldstein and P. Meystre, Phys. Rev. A **59**, 3896 (1999).

[29] T. Ohmi and K. Machida, J. Phys. Soc. Japan **67**, 1882 (1998).

[30] T.-L. Ho, Phys. Rev. Lett. **81**, 742 (1998).

[31] D. F. Walls and G. J. Milburn, *Quantum Optics* (Springer-Verlag, Berlin, 1994).

[32] M. Moriga, M. Yasuda, T. Kishimoto, and F. Shimizu, Phys. Rev. Lett. **77**, 802 (1996).

[33] A. Soroko, J. Phys. B **30**, 5621 (1997).

[34] F. Dalfovo, S. Giorgini, L. P. Pitaevskii, and S. Stringari, Rev. Mod. Phys. **71**, 513 (1999).

[35] O. Zobay, E. V. Goldstein, and P. Meystre, Phys. Rev. A in press (1999).